Available online at www.sciencedirect.com

jmr&t Journal of Materials Research and Technology

journal homepage: www.elsevier.com/locate/jmrt

Short Communication

Microstructure and mechanical response of novel Co-free FeNiMnCrAlTi high-entropy alloys

Roghayeh Mohammadzadeh [a], *Akbar Heidarzadeh* [a,*], *H. Tarık Serindağ* [b], *Gürel Çam* [c]

[a] *Department of Materials Engineering, Azarbaijan Shahid Madani University, Tabriz, Iran*
[b] *Department of Aerospace Engineering, Iskenderun Technical University, Iskenderun-Hatay, Turkey*
[c] *Department of Mechanical Engineering, Iskenderun Technical University, Iskenderun-Hatay, Turkey*

ARTICLE INFO

Article history:
Received 11 June 2023
Accepted 6 August 2023
Available online 10 August 2023

Keywords:
Co-free high-entropy alloy
Homogenizing
Hot rolling
Ductile fracture

ABSTRACT

The present study investigates the microstructure and mechanical properties of the Co-free FeNiMnCrAlTi high-entropy alloy (HEA) after casting, homogenizing heat treatment, and hot rolling. The results show that the dendrite regions in the as-cast state were enriched in Cr and Fe and inter-dendritic regions were saturated with Ti and Al. By homogenizing heat treatment, the dendritic solidification structure is eliminated. Furthermore, the microstructure was refined after hot rolling. The EDS and XRD analyses show that despite the matrix and secondary phases' different chemical compositions, their crystal structures are the same. The as-rolled HEA revealed an excellent compromise in mechanical properties: 720 MPa yield strength, 922 MPa ultimate tensile strength, and 30% elongation. A typical ductile failure was observed on the fracture surface of the as-rolled HEA.

1. Introduction

Among HEAs, an equiatomic single-phase face-centered cubic (fcc) CoCrFeMnNi HEA shows high ductility, superior corrosion resistance, and exceptional thermal stability [1,2]. Although the fcc-structured HEAs show superior mechanical performance at cryogenic temperatures, they still could not be used in future structural applications due to their low yield strength [3]. Therefore, designing HEAs with a good combination of strength and ductility for practical demands is still challenging.

Several studies have been performed to enhance the strength of fcc-structured HEAs. Precipitate-forming elements such as Al, Ti, Nb, and Mo have been demonstrated to enhance the yield strength of the CoCrFeNi-based HEAs by the precipitation-strengthening mechanism [4,5]. Qi et al. [4] added the Al and Ti elements to the CoCrFeNi matrix and found that the CoCrFeNi$(Al_{0.3}Ti_{0.2})_{0.5}$ exhibited a yield strength of 820 MPa and elongation of 20%. Fan et al. [5] studied the effect of Nb and Mo on the mechanical properties of CoCrFeNi-(Nb, Mo) HEAs and found that the precipitation and solid-solution strengthening enhanced the yield strength up to 426 MPa while maintaining high elongation (17%).

* Corresponding author.
E-mail addresses: ac.heydarzadeh@azaruniv.ac.ir, ak.hz62@gmail.com (A. Heidarzadeh).
https://doi.org/10.1016/j.jmrt.2023.08.039

But, the high cost of Co element in fcc-structured HEAs is a practical issue. As it is known, the price of the Co element is almost 3 times higher than that of the Ni element [6]. Therefore, the development of Co-free HEAs with well-balanced mechanical performance is highly desired. The FeNiCrMn alloy exhibits a face-centered-cubic structure and good ductility like the CoCrNi and CoCrFeNi alloys making it a potential candidate in engineering applications [7]. However, the yield and ultimate strength of the FeNiMnCr alloy are very low at room temperature, which is 250 and 600 MPa, respectively [8]. The Co-free FeNiMnCr alloy could be strengthened by forming a multi-phase structure or precipitation [9,10]. If the hard phase could form in the fcc-structured FeNiMnCr matrix, the Co-free HEAs with a good high ductility and strength balance can be obtained. In order to achieve this aim, a Co-free FeNiMnCrAlTi HEA was designed and prepared in this study. The microstructural evolution and mechanical behaviors of this novel Co-free HEA were investigated systematically.

2. Experimental

An ingot of Co-free HEA with a composition of $Fe_{37.06}Ni_{30.47}Mn_{12.44}Cr_{12.00}Al_{4.01}Ti_{4.01}$ was prepared by vacuum arc melting furnace with high purity meals (99.9%). The ingot was re-melted 5 times and prepared in the form of a slab with a weight of 200 g and dimension of 13.5 × 2.5 × 1.5 cm^3. The as-cast HEA was homogenized at 1100 °C for 48 h in a muffle furnace and then hot rolled at 1000 °C to achieve a thickness of 2.5 mm. Four samples with a size of 20 × 20 × 2.5 mm^3 were cut from the as-cast, as-homogenized, and as-rolled alloy and ground, polished, and subsequently etched using a solution of HCl and HNO_3 with a volume ratio of 1:3. The phase constituents were determined by Empyrean X-ray diffractometer (XRD) at 45 kV and 40 mA using a Cu K_α radiation. The XRD patterns were acquired over a $2\theta = 20°–90°$ using a scanning step of 0.05° and a time step of 594 s. The microstructure of the samples was characterized by optical microscopy (OM, JENUS model) and field-emission gun scanning electron microscope (FESEM, Apreo 2S, ThermoFisher Scientific) equipped with an energy dispersive spectroscope (EDS).

Flat tensile samples (with gauge length, width, and thickness of 20 mm, 12.5 mm, and 2 mm, respectively) were prepared according to the JIS Z 2201 standard and tested at room temperature with a tensile speed of 0.2 mm min^{-1}. Tension tests were performed with a universal tensile test machine (SUT-50, Sanaf Co, Iran) and three repeat tests were conducted.

3. Results and discussion

3.1. Microstructure of as-cast and as-homogenized HEA

Figs. 1 and 2 illustrate the microstructure of the as-cast and as-homogenized HEA. Fig. 1 reveals the presence of dendritic patterns in the as-cast structures. Based on the EDS results, it has been observed that the interdendritic region has a high concentration of Ti and Ni elements, while the dendrite region contains a significant amount of Fe and Cr elements. The separation of elements in HEAs can be clarified by the interplay of mixing enthalpies between the metal elements. Due to the comparatively higher positive enthalpy of Ti with Fe and Cr, it is pushed away from the dendrite region by these

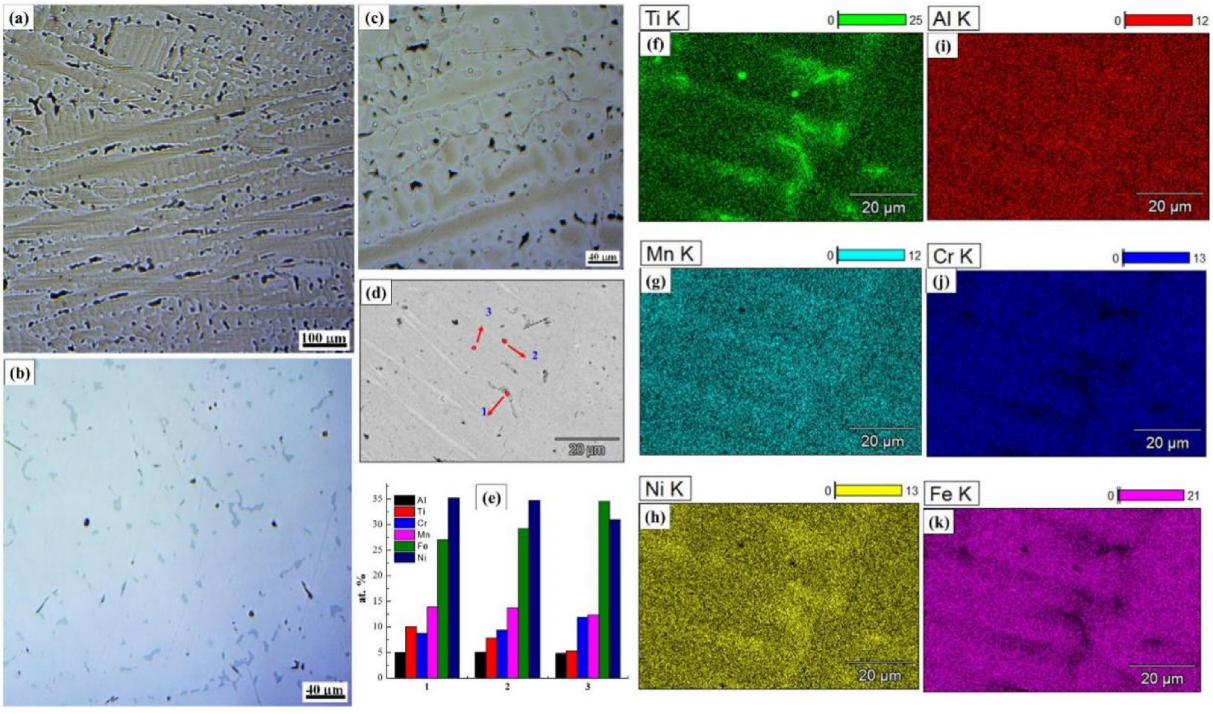

Fig. 1 – Microstructure of as-cast HEA in the (a, c) as-etched (b) as-polished condition (d) SEM image, (e) EDS analysis results of point 1, 2 and 3, and (f–k) EDS maps.

elements. In contrast, Mn and Al display lower positive enthalpies with Ti, which causes them to be partially drawn toward the interdendritic region.

The OM images confirm the complete disappearance of the dendritic structure and the emergence of grains and twin boundaries after homogenizing (as shown in Fig. 2(a) and (b)). It is also evident that the secondary phase did not undergo any significant changes after the homogenizing (Fig. 2(c) and (d) the secondary phases are enriched with Ti, Al, and Ni elements while being deficient in Fe and Cr elements (Fig. 2(f)–(k)). The segregation ratio values of Ti, Al, and Ni between the secondary phases and the matrix were found to be 3.3, 5.5, and 1.6, respectively. The changes in the segregation ratio can be attributed to the difference in melting temperatures between Al and other elements, as well as the highly negative values of enthalpy mix (ΔH_{mix}) of the Al–Ni (−66.3 ± 1.7 kJ/mol) [11] and Al–Ti (−30 kJ/mol) solid solutions [12].

3.2. *Microstructural evolution during deformation*

The microstructure of the as-hot rolled HEA is displayed in Fig. 3, which shows fine equiaxed grains along with twins, indicating the heavy deformation of the alloy. Grain refinement is also evident after the hot rolling. Fine microstructure with a mean grain size of 20 μm is formed in a hot rolled plate. Further observation of the microstructure using OM images at high magnification (Fig. 3(b) and (c)) reveals the presence of secondary phases within the microstructure. Mn element was still distributed uniformly, while elements Ti, Al, Fe, Cr, and somewhat Ni were not (Fig. 3(f)–(k)). The secondary phases were enriched in Ti and Al elements, indicating their contribution to the formation of the secondary phases.

The XRD patterns of the as-homogenized and as-rolled HEAs are shown in Fig. 4 (a), revealing that both alloys have reflections of a single face-centered-cubic (FCC) solid solution phase, providing further support for the accuracy of the OM and SEM analyses. However, the intensities of the peaks ascribed to the planes of the FCC phase changed after hot rolling. The (220) peak weakened, while the (111), (200), (311), and (222) peaks strengthened compared to the as-homogenized HEA.

These changes in peak intensities were generally associated with the texture evolution during rolling. It should be noted that XRD patterns did not exhibit reflections from the secondary phase, indicating that the peaks from the secondary phase are similar to those from the matrix, and the peaks of the secondary phase may overlap with the matrix or be too small to be distinguished. In contrast, Zhao et al. [9] reported the presence of nanosized particles in Co-free HEAs. The reason for this is probably the aging treatment they conducted after cold rolling.

3.3. *Tensile properties at room temperature*

Fig. 4 (b) displays the representative stress-strain curve for the as-rolled HEA, indicating a yield strength of 720 MPa, ultimate strength of 922 MPa, and elongation of 30%. The high yield and ultimate tensile strengths are likely due to solid-solution effects resulting from the alloy's additions of Fe, Mn, Ni, Cr, Ti, and Al, as well as the presence of a secondary phase enriched in Ti and Al. In Fig. 4c, the tensile fracture surfaces of the as-rolled HEA are displayed, demonstrating numerous dimples that are characteristic of ductile fracture features. In general, ductile fracture arises due to the formation and coalescence of microvoids ahead of the cracks. As microvoids appear in the

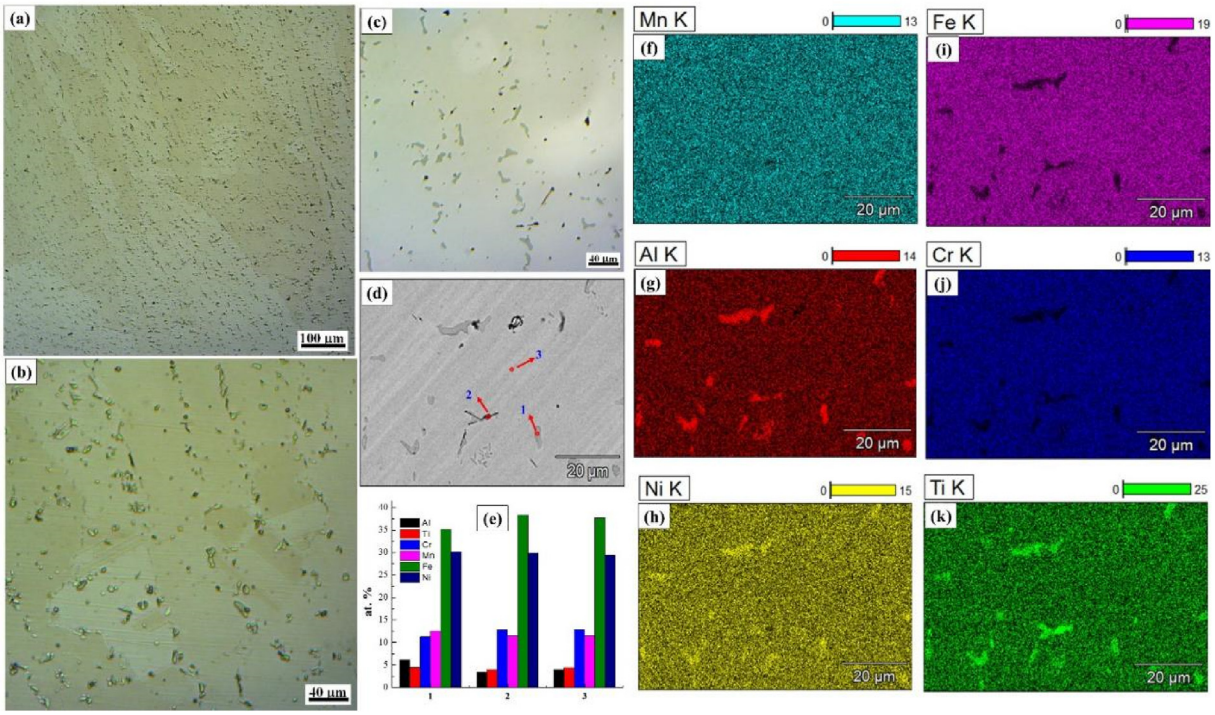

Fig. 2 – Microstructure of as-homogenized HEA in the (a, b) as-etched (c) as-polished condition (d) SEM image, (e) EDS analysis results of point 1, 2, and 3, and (f–k) EDS maps.

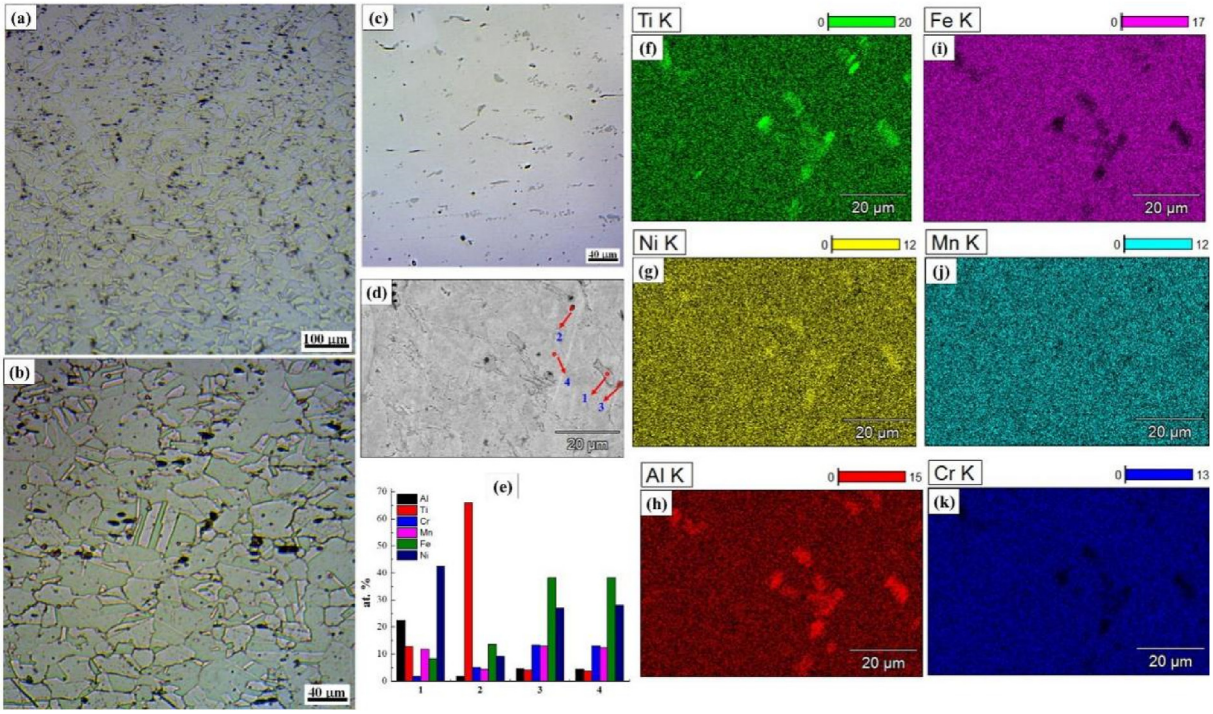

Fig. 3 – Microstructure of as-rolled HEA in the (a, b) as-etched, (c) as-polished condition, (d) SEM image, (e) EDS analysis results of point 1, 2, and 3, and (f–k) EDS maps.

alloy during plastic deformation, primarily on the surfaces of phases, they join together. The final fracture occurs when the walls between these growing voids break. The fracture surfaces of this ductile HEA are distinguished by excessive plastic deformation and the formation of a rough fracture surface with deep dimples.

Backscattered electrons (BSE) and EDX mapping analysis were employed to enhance and achieve the identification of

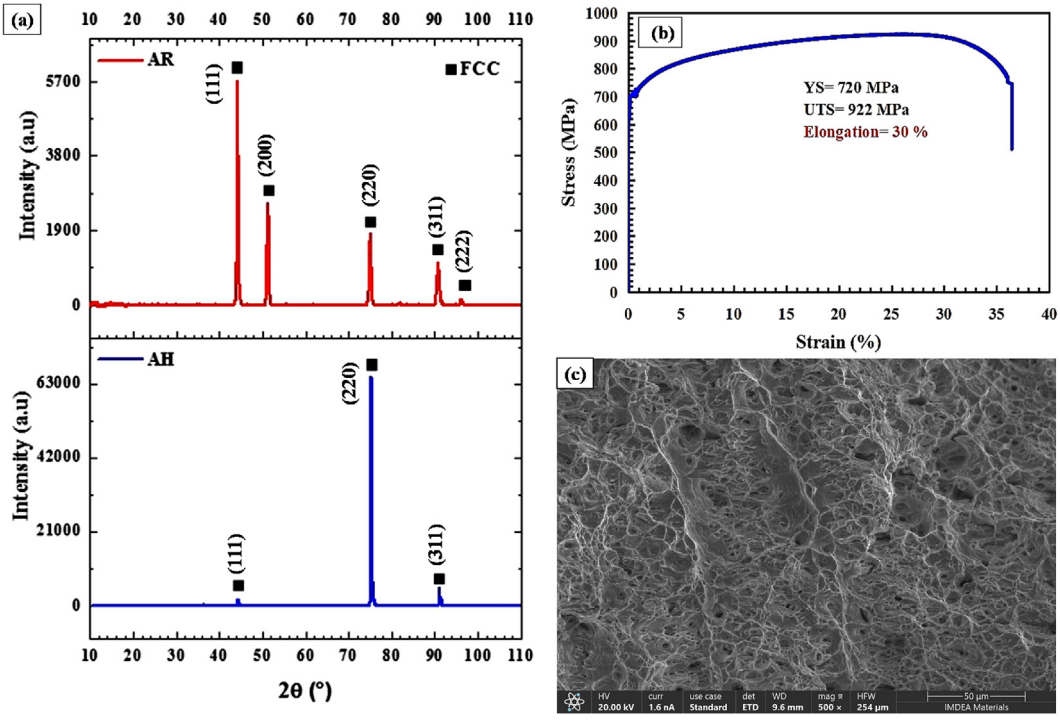

Fig. 4 – (a) XRD patterns of the as-homogenized (AH) and as-rolled (AR) Co-free HEA, (b) tensile stress-strain curve of as-rolled HEA at room temperature, and (c) tensile fracture surface showing ductile dimple fracture.

microstructural features on the fracture surfaces. Fig. 5 shows the SEM images with Al, Cr, Fe, Ni, Mn, and Ti mapping on the fracture surfaces of as-rolled HEA. The EDX images seem to highlight a more intense color in different regions (see Fig. 5c). This is an expected result and it is most likely due to the presence of secondary phases. It is interesting to note that, according to the data of line scanning along dimples (Fig. 5c), dimples were evident along with Al, Ni, and Ti on the fracture surface, which indicates that a failure possibly occurred during the tensile test within the matrix near the interface between the matrix and secondary phases enriched in Al, Ni, Ti.

In Fig. 6, a direct comparison is made between the tensile properties (ultimate tensile strength and elongation) of the current Co-free HEA and different Co-free HEAs reported in references [9–19]. The properties of previously studied Co-free HEAs are contained within the blue envelope, indicating a significant compromise between strength and ductility. In contrast, our newly developed Co-free HEA effectively breaks away from this trade-off and demonstrates an exceptional combination of strength and ductility. However, the tensile strength value obtained in this study is quite lower than that reported by Zhao et al. [9] for Co-free HEA which was produced by casting in an arc-melting furnace and subsequent thermo-mechanically processing followed by solution treatment, cold rolling, and finally an aging treatment. The Co-free HEAs produced in such a way exhibited very high tensile strength (i.e. over 1 GPa) and a still good elongation (minimum about 30%). The tensile elongation values obtained in the current study are, on the other hand, similar to those reported by Zhang et al. [7]. Although the tensile strength they reported is superior to that of the current study they used a 5-stage production including cold rolling and aging treatments. In comparison, a 3-stage processing consisting of melting, homogenization, and hot rolling was used in the current study. This was believed to be the reason for obtaining lower tensile strength values. However, even so, the tensile strength obtained is reasonably high compared to those of the HEAs reported in the literature as shown in Fig. 6.

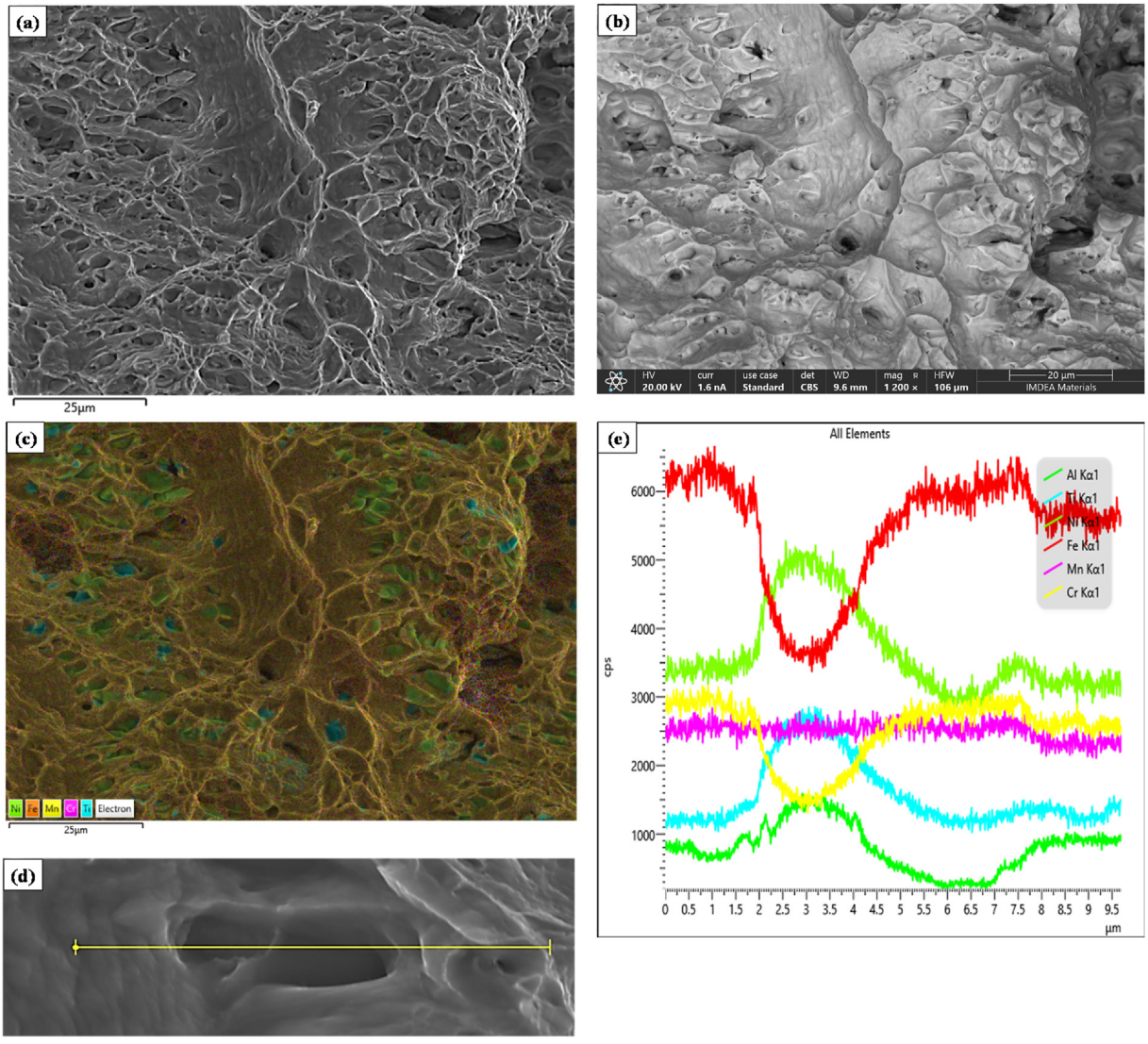

Fig. 5 – SEM image of the fracture surface using secondary electrons (a), backscattered (b), EDS (element mapping); overlay images at the fracture surface (c), and line EDS analysis along dimples (d, e).

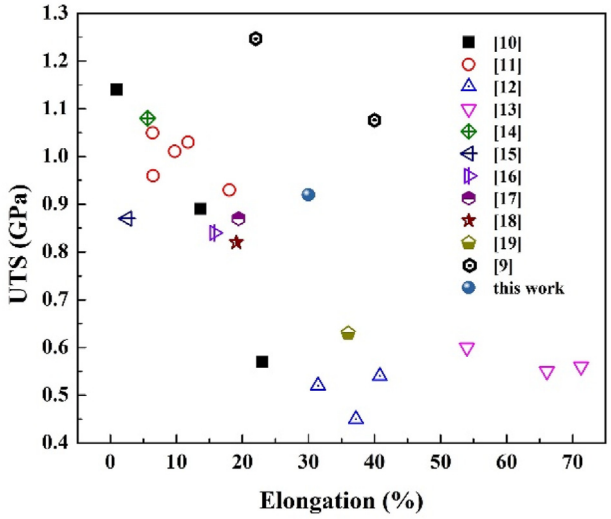

Fig. 6 – Summary of tensile characteristics obtained from different Co-free HEA, indicating a great advantage of the present HEA.

4. Conclusion

A Co-free FeNiMnCrAlTi HEA was produced through vacuum induction melting of high-purity raw materials. The microstructure and mechanical properties were examined at different stages of processing, namely as-cast, as-homogenized, and as-rolled. The following conclusions could be drawn from this research.

1. The Co-free HEA exhibited a dendritic solidification microstructure in the as-cast condition. The homogenizing heat treatment at 1100 °C for 48 h, successfully breaks up the dendritic solidification microstructure and alleviates the micro-segregation, producing a microstructure comprised of coarse fcc-structured grains and a secondary phase.
2. The combination of fine fcc-structured grains and secondary phase led to an excellent compromise between strength and ductility, and the alloy revealed a tensile strength of 922 MPa, yield strength of 720 MPa, and elongation of 30%.
3. The as-rolled HEA fractography showed a typical ductile fracture with dimples.

Data availability

Data will be available on request.

Declaration of competing interest

The authors declare that they have no known competing financial interests or personal relationships that could have appeared to influence the work reported in this paper.

Acknowledgment

This study was supported by the University of Tabriz, the International Academic Cooperation Center of the Iranian Ministry of Science, Research and Technology (MSRT) (grant/contraction number: IRTU-2-1406), and the Scientific and Technological Research Council of Turkey (TÜBİTAK) (project number: 121N242) within second call of MSRT-TÜBİTAK joint research projects.

REFERENCES

[1] Kaushik N, Meena A, Mali HS. High entropy alloy synthesis, characterisation, manufacturing & potential applications: a review. Mater Manuf Process 2022;37. https://www.tandfonline.com/doi/full/10.1080/10426914.2021.2006223.
[2] Mohammadzadeh A, Heidarzadeh A, Becker H, Robles JV, Meza A, Avella M, et al. Exploring the Impact of Configurational Entropy on the Design and Development of CoNi-Based Superalloys for Sustainable Applications. J Alloys Compd 2023 Jul;14:171380. https://www.sciencedirect.com/science/article/pii/S092583882302683X.
[3] Lu K, Chauhan A, Litvinov D, Tirunilai AS, Freudenberger J, Kauffmann A, et al. Micro-mechanical deformation behavior of CoCrFeMnNi high-entropy alloy. J Mater Sci Technol 2022;100:237–45. https://www.sciencedirect.com/science/article/pii/S1005030221005818.
[4] Qi W, Wang W, Yang X, Zhang G, Ye W, Su Y, et al. Effects of Al and Ti co-doping on the strength-ductility-corrosion resistance of CoCrFeNi-AlTi high-entropy alloys. J Alloys Compd 2022;925:166751. https://www.sciencedirect.com/science/article/pii/S0925838822031425.
[5] Fan R, Wang L, Zhao L, Wang L, Zhao S, Zhang Y, et al. Synergistic effect of Nb and Mo alloying on the microstructure and mechanical properties of CoCrFeNi high entropy alloy. Mater Sci Eng, A 2022;829:142153. https://www.sciencedirect.com/science/article/pii/S0921509321014179.
[6] Lu Y, Zhang K, Zhao B, Dong X, Zhang L. A comparative study of two C-containing high-entropy alloys Al0. 3CrFeNi2 and Al0. 3CoCrFeNi. Mater Sci Eng, A 2022;853:143702. https://www.sciencedirect.com/science/article/pii/S0921509322010863.
[7] Zhang Y, Wu H, Yu X, Tang D, Yuan R, Sun H. Microstructural evolution and strengthening mechanisms in CrxMnFeNi high-entropy alloy. J Mater Res Technol 2021;12:2114–27. https://www.sciencedirect.com/science/article/pii/S2238785421003641.
[8] Wu Z, Bei H. Microstructures and mechanical properties of compositionally complex Co-free FeNiMnCr18 FCC solid solution alloy. Mater Sci Eng, A 2015;640:217–24. https://www.sciencedirect.com/science/article/pii/S0921509315300435.
[9] Zhao YL, Yang T, Zhu JH, Chen D, Yang Y, Hu A, et al. Development of high-strength Co-free high-entropy alloys hardened by nanosized precipitates. Scripta Mater 2018;148:51–5. https://www.sciencedirect.com/science/article/pii/S1359646218300551.
[10] Dębski A, Gąsior W, Sypień A, Góral A. Enthalpy of formation of intermetallic phases from Al–Ni and Al–Ni–Ti systems. Intermetallics 2013;42:92–8.
[11] Men H, Zhongyun F. An analytical model for solute segregation at liquid metal/solid substrate interface. Metall Mater Trans 2014;45:5508–16.

[12] Wang Z, Wu M, Cai Z, Chen S, Baker I. Effect of Ti content on the microstructure and mechanical behavior of (Fe36Ni18Mn33Al13) 100− xTix high entropy alloys. Intermetallics 2016;75:79–87. https://www.sciencedirect.com/science/article/pii/S0966979516300565.

[13] Meng F, Qiu J, Baker I. The effects of chromium on the microstructure and tensile behavior of Fe30Ni20Mn35Al15. Mater Sci Eng, A 2013;586:45–52. https://www.sciencedirect.com/science/article/pii/S0921509313008666.

[14] Wang Z, Baker I. Interstitial strengthening of an fcc FeNiMnAlCr high entropy alloy. Mater Lett 2016;180:153–6. https://www.sciencedirect.com/science/article/pii/S0167577X16308886.

[15] Stepanov ND, Shaysultanov DG, Tikhonovsky MA, Salishchev GA. Tensile properties of the Cr–Fe–Ni–Mn non-equiatomic multicomponent alloys with different Cr contents. Mater Des 2015;87:60–5. https://www.sciencedirect.com/science/article/pii/S0264127515302574.

[16] Ng C, Guo S, Luan J, Wang Q, Lu J, Shi S, et al. Phase stability and tensile properties of Co-free Al0. 5CrCuFeNi2 high-entropy alloys. J Alloys Compd 2014;584:530–7. https://www.sciencedirect.com/science/article/pii/S0925838813022688.

[17] Shaysultanov DG, Salishchev GA, Ivanisenko YV, Zherebtsov SV, Tikhonovsky MA, Stepanov ND. Novel Fe36Mn21Cr18Ni15Al10 high entropy alloy with bcc/B2 dual-phase structure. J Alloys Compd 2017;705:756–63. https://www.sciencedirect.com/science/article/pii/S0925838817306576.

[18] Wu M, Munroe PR, Baker I. Martensitic phase transformation in a fcc/B2 FeNiMnAl alloy. J Mater Sci 2016;51:7831–42. https://link.springer.com/article/10.1007/s10853-016-0015-4.

[19] Baker I, Meng F, Wu M, Brandenberg A. Recrystallization of a novel two-phase FeNiMnAlCr high entropy alloy. J Alloys Compd 2016;656:458–64. https://www.sciencedirect.com/science/article/pii/S0925838815312482.